A Consistent Level Set Formulation for Large-Eddy Simulation of Premixed Turbulent Combustion

H. Pitsch

Department of Mechanical Engineering, Stanford University, Stanford, CA 94305-3030

Abstract

A consistent formulation of the G-equation approach for LES is developed. The unfiltered G-equation is valid only at the instantaneous flame front location. Hence, in a filtering procedure applied to derive the appropriate LES equation, only the instantaneous unfiltered flame surface can be considered. A new filter kernel is provided, which averages along the flame surface. The filter kernel is used to derive the G-equation for the filtered flame front location. This equation has two unclosed terms, involving a flame front conditional averaged flow velocity, and a filtered propagation term. A model for the conditional velocity is derived, expressing this quantity in terms of the Favre-filtered flow velocity, which is typically known from a flow solver. This model leads to the appearance of a density ratio in the propagation term of the G-equation. LES of combustion in the thin reaction zones regime is discussed in the LES regime diagram. A new line is identified separating the thin reaction zones regime into two parts, where the broadended flame thickness is larger and smaller than the filter size, respectively. A model for the propagation term is provided. This leads to a term including the sub-filter turbulent burning velocity and an additional term proportional to the resolved flame front curvature. For the former, an algebraic model is provided from an equation for the sub-filter flame front wrinkling. The latter term depends on the inverse of the sub-filter Damköhler number and disappears in the corrugated flamelets regime.

Key words: premixed turbulent combustion, large-eddy simulation, level set method, regime diagram
PACS:

Email address: H.Pitsch@stanford.edu (H. Pitsch).

1 Introduction

Premixed turbulent combustion in technical devices often occurs in thin flame fronts. The propagation of these fronts, and hence also the heat release, are governed by the interaction of transport processes and chemistry within the front. In flamelet models, this strong coupling is expressed in treating the flame front as a thin interface propagating with a laminar burning velocity s_L. The coupling of transport and chemistry is reflected in the scaling of the laminar burning velocity, which can be expressed as $s_L \sim \sqrt{D/t_c}$, where D is the diffusion coefficient and t_c is the chemical time scale. Flamelet models for premixed turbulent combustion have been extensively used in the past and different models have been formulated for Reynolds averaged [1, 2] and large-eddy simulation (LES) [3–9] methods.

Most of the combustion models proposed for LES of premixed and non-premixed turbulent combustion are similar to RANS models. But LES poses some additional challenges, especially for applications to premixed combustion problems. One of the main challenges is caused by the thinness of flames in many technical devices compared with the geometrical scales and the large scales of the turbulence. For thin flames, the instantanous temperature field is essentially discontinuous, but the flame will be at different locations at different times. The flame brush thickness is typically on the order of the integral scale of the turbulence, and the Reynolds averaged temperature field will vary smoothly over that distance. As long as a computational mesh resolves the integral scale of the turbulence, which is already a requirement for resolving the mean velocity field, thin flames pose no problems in a RANS type approach. In LES, the equations for the spatially filtered fields are solved without any ensemble or time averaging. The filter width is typically chosen such that only the large-scale, energy-containing part of the turbulence is resolved. The consequence is that, if the flame is thin compared to the integral scale of the turbulence, and specifically, if the flame is thin compared with the size of the filter, the change of the temperature from its unburned to its burned value occurs on a spatial scale smaller than the filter width. It will be shown below that this is the case, if the sub-filter Damköhler number is smaller than unity. At present, LES of combustion is performed using implicit filtering, which means that the spacing of the computational discretization coincides with the filter width. The change of the temperature from unburned to burned will hence be resolved with just one computational cell, which, from a numerical point of view, is very challenging. Hence, if models are used which are based on the solution of filtered equations of reactive scalars, such as the temperature or a reaction progress variable, a special treatment of the discontinuity is required. The correct procedure of using explicit filtering, however, seems to be computationally infeasible. Even if the change of the filtered temperature from the unburned to the burned value was resolved by only ten computational cells,

a simulation would require meshes that are larger by at least three orders of magnitude. This problem is similar to solving for shocks in supersonic flows, where special techniques, such as front capturing and front tracking, have been developed for adequately handling such discontinuities in the solution. If such techniques are not applied, the solution is poisoned by numerical diffusion, which will substantially modify effective propagation velocities. Interestingly, this issue is less important for the momentum equations, since for these equations the conserved quantity varies smoothly across the flame. However, the flux of momentum appearing in the convection term jumps across the flame, which can lead to numerical stability problems.

An alternative, where the front propagation is not described by the solution of reactive scalar equations, is the use of the so called G-equation. The G-equation model proposed by Williams [10] is based on the flamelet modeling assumptions and uses a level set method to describe the evolution of the flame front as an interface between the unburned and burned gases. The level set function G is a scalar field defined such that the flame front position is at $G = G_0$, and that $G < G_0$ in the unburned mixture. The G-equation describes the evolution of an interface associated with the flame front as a level set function that is continuous through the flame front even for infinitely thin flames. This method therefore does not suffer from the numerical issues described above.

The instantaneous and local G-equation can be derived by considering the instantaneous flame surface. The derivation is described elsewhere [2, 10], but has to be sketched briefly in the following for clarity. An implicit representation of the instantaneous flame surface can be given as

$$G(\boldsymbol{x_f}, t) - G_0 = 0\,, \tag{1}$$

which defines the level set function G. Here, t is the time and $\boldsymbol{x_f}$ is the flame front location. Differentiating Eq. (1), one obtains

$$\frac{\partial G}{\partial t} + \frac{d\boldsymbol{x_f}}{dt} \cdot \nabla G = 0\,. \tag{2}$$

If the curvature radius of the instantaneous flame front is locally larger than the flame thickness, the flame is in the corrugated flamelets regime, and the flame front propagation speed is given by

$$\frac{d\boldsymbol{x_f}}{dt} = \boldsymbol{v} + s_L \boldsymbol{n}\,, \tag{3}$$

where $\boldsymbol{v}$ is the local flow velocity and s_L is the laminar burning velocity. Note that this may differ from the unstrained laminar burning velocity s_L^0 because

of the flame geometry. It is well known, for instance, that front propagation leads to the formation of cusps in the flame surface. These cusps form singular points, where the propagation speed is higher than s_L^0.

The flame normal vector $\boldsymbol{n}$ is defined to be directed into the unburned and can be expressed as

$$\boldsymbol{n} = -\frac{\nabla G}{|\nabla G|}\,. \tag{4}$$

Combining Eqs. (2) and (3) yields the instantaneous G-equation

$$\frac{\partial G}{\partial t} + \boldsymbol{v}\cdot\nabla G = s_L\,|\nabla G|\ . \tag{5}$$

Since this equation has been derived from Eqs. (1) and (3), which both only describe the flame surface, also Eq. (5) is valid at the flame surface only. The remaining G-field is arbitrary and commonly defined to be a distance function.

The location of G_0 can be defined to be anywhere in the flame, for instance at a given temperature iso-surface. Then, in Eq. (5), the velocity $\boldsymbol{v}$ is evaluated at that location, and the laminar burning velocity s_L has to be defined with respect to that location as well. Typically, G_0 is defined to be either immediately ahead of the flame in the unburned, or immediately behind the flame in the burned gases. The burning velocities defined with respect to the unburned and burned gases are denoted as $s_{L,u}$ and $s_{L,b}$, respectively.

Peters [2, 11, 12] has developed an appropriate theory describing premixed turbulent combustion in the corrugated flamelets and the thin reaction zones regimes based on the G-equation formulation. Peters [2] and Oberlack et al. [13] pointed out that, since the G-field has physical meaning only at $G = G_0$, in order to derive the Reynolds averaged G-equation, conventional ensemble or time averaging of the G-field cannot be applied. For LES, this implies not only that is it impossible to obtain a filtered G-field from filtering the instantaneous resolved field, but also that the filter kernels, that are used for filtering the velocity and scalar fields cannot be applied. In the application of the G-equation in LES, these facts have not been considered in the past. Hence, we first need to develop a filter kernel that takes information only from the instantaneous resolved flame surface. This will be done in the next section. Thereafter, the equation for the filtered flame front position in the corrugated flamelets regime will be derived. The resulting equation has two unclosed terms, a flame front conditionally averaged flow velocity appearing in the convection term, and the sub-filter burning velocity. To relate the conditional velocity to the unconditionally filtered velocity, which is known from the solution of the momentum equations, a model for this quantity applicable

in the corrugated flamelets regime will be developed in section 3. In section 4, the filtered G-equation for the thin reaction zones regime will be derived. In addition to the resolved parts of the burning velocity, two different contributions to the sub-filter burning velocity will be identified. One represents the sub-filter contributions from the corrugated flamelets and the thin reaction zones regime, the other one accounts for the interaction of sub-filter turbulent transport with the resolved flame front curvature. These contributions will be modeled separately. Before deriving models for the individual contributions to the sub-filter burning velocity, LES specific issues will be discussed using an LES regime diagram, which is similar to that proposed by Pitsch and Duchamp [6], but includes a new line important for the closure of the equation describing the filtered flame front. Finally, we will derive an equation for the sub-filter flame front wrinkling, which will lead to an analytic model for the sub-filter contribution to the sub-filter burning velocity.

2 Definition of the filtered flame front location

Peters [2] and Oberlack et al. [13] have pointed out that for the derivation of a G-equation describing the ensemble or time averaged flame location the traditional averaging of the G-field cannot be applied. Because the G-field has physical significance only for $G = G_0$, only the G_0 iso-surface can be of relevance in the averaging procedure. The remaining G-field, which can be arbitrarily defined, must not be used. Instead, Peters [2] has proposed an averaging procedure that only uses the probability density function (pdf) of finding $G = G_0$ at a particular location. This procedure was described only for the one-dimensional case. Oberlack et al. [13] developed a rigorous ensemble averaging procedure for the three-dimensional case. Through the consistent application of this averaging procedure, a G-equation for the averaged flame location and an equation for the flame brush thickness have been derived for the corrugated flamelets regime.

In this section, we will first propose an appropriate LES filter, which will be used to derive a level set equation for the filtered flame front location in the corrugated flamelets regime by using similar arguments as given by Oberlack et al. [13]. The resulting G-equation will be extended to the thin reaction zones regime in a following section.

Several definitions of filter kernels that define sub-filter surface averaged quantities are possible. The ideal filter is a projection filter operation that commutes with the temporal and spatial derivatives. Both of these properties are non-trivial to achieve for practical definitions. Note however that for the purpose of the present study, it would be sufficient to just assume a filtering operation with certain properties. The results are not dependent on the exact definition

of the filtering procedure. This only has to be known, for instance, in the formulation of dynamic models, where an explicit filtering is necessary.

A possible surface averaging technique has been provided by Pope [14], and an extension to LES was formulated by Hawkes [15]. This filtering method is very similar to the method proposed here, but the resulting filtered quantity is a function of space. Apparently, this cannot be applied to compute a flame surface averaged front position, which is not a field quantitiy. The method presented below leads to a parameter representation of the filtered front. Another possibility is the use of the conditional filtering method introduced by Colucci et al. [16], where G is the conditioning variable. The filtered flame front position could then be determined as the filtered front position conditioned on $G = G_0$. This, however, also leads to a field quantity and can therefore not be used.

A parametric representation of the flame surface $\mathbf{F}$ can be given as

$$\boldsymbol{x_f} = \boldsymbol{x_f}(\lambda, \mu, t)\,, \tag{6}$$

where $\boldsymbol{x_f}$ is the flame front location, and λ and μ are curvilinear coordinates along the flame surface forming an orthogonal coordinate system moving with the flame front. Considering a point P_0 on the flame surface, which is given by the coordinates (λ_0, μ_0), $\boldsymbol{x_f}(\lambda_0, \mu_0, t)$ describes the temporal development of the location of the point P_0 in physical space as function of time t. The coordinates λ and μ are hence parameters of the function $\boldsymbol{x_f}$ and will in the following be written as $\mathbf{\Lambda} = \binom{\lambda}{\mu}$.

For a given set of parameters $\mathbf{\Lambda}$, a spatial filter $\mathbf{H}$ can then be defined as

$$\mathbf{H}\left(\mathbf{\Lambda} - \mathbf{\Lambda}', t\right) = \begin{cases} M(\mathbf{\Lambda}, t)/S(\mathbf{\Lambda}, t), & \text{if } \left|\boldsymbol{x_f}\left(\mathbf{\Lambda}\right) - \boldsymbol{x_f}\left(\mathbf{\Lambda}'\right)\right| \leq \frac{\mathbf{\Delta}}{2} \\ 0, & \text{otherwise} \end{cases}\,, \tag{7}$$

where $\mathbf{\Delta}$ is the filter width, and

$$M(\mathbf{\Lambda}, t) = \left| \frac{\partial \boldsymbol{x_f}}{\partial \lambda} \times \frac{\partial \boldsymbol{x_f}}{\partial \mu} \right|\,. \tag{8}$$

$1/S(\mathbf{\Lambda}, t)$ is a factor that is determined by the normalization condition

$$\int\limits_{\mathbf{F}} \mathbf{H}\left(\mathbf{\Lambda} - \mathbf{\Lambda}', t\right) d\mathbf{\Lambda}' = 1\,. \tag{9}$$

Physically, $M d\lambda d\mu$ represents a differential element of area and S is the area

of the flame within the filter. This filter function is substantially different from the conventionally applied filter kernels for scalar quantities. Since the flame is only defined on a surface, the filter also has to move along this surface and cannot be used at an arbitrary point in space. The coordinates used in the filter function are therefore not spatial, but flame surface coordinates. Then, a spatial filtering operation for the flame front location can be defined as

$$\widehat{\boldsymbol{x}}_f\left(\boldsymbol{\Lambda},t\right)=\int\limits_{\mathbf{F}}\boldsymbol{x_f}\left(\boldsymbol{\Lambda'},t\right)\mathbf{H}\left(\boldsymbol{\Lambda}-\boldsymbol{\Lambda'},t\right)d\boldsymbol{\Lambda'}\,. \tag{10}$$

This filtering operation is sketched in Fig. 1 for the two-dimensional case and will be described in more detail for clarity. The surface coordinates $\boldsymbol{\Lambda}$ are defined along the instantaneous flame surface. To obtain the filtered front location, for each point $\boldsymbol{x_f}(\boldsymbol{\Lambda})$ on the instantaneous flame surface, the filtering operation Eq. (10) yields a corresponding mean flame front location $\widehat{\boldsymbol{x}}_f(\boldsymbol{\Lambda})$. These locations $\widehat{\boldsymbol{x}}_f(\boldsymbol{\Lambda})$ define the filtered flame front position.

3 *G*-Equation for the filtered flame location valid in the corrugated flamelets regime

For the derivation of the level set equation for the filtered flame front location, the filtering operation is first applied to Eq. (3), which leads to

$$\widehat{\frac{d\boldsymbol{x_f}}{dt}}=\widehat{\boldsymbol{v}}+\widehat{s_L\boldsymbol{n}}\,. \tag{11}$$

The conditionally filtered flow velocity and propagation term appearing in this equation are given by

$$\widehat{\boldsymbol{v}}\left(\boldsymbol{\Lambda},t\right)=\int\limits_{\mathbf{F}}\boldsymbol{v}\left(\boldsymbol{\Lambda'},t\right)\mathbf{H}\left(\boldsymbol{\Lambda}-\boldsymbol{\Lambda'},t\right)d\boldsymbol{\Lambda'} \tag{12}$$

and

$$\widehat{s_L\boldsymbol{n}}\left(\boldsymbol{\Lambda},t\right)=\int\limits_{\mathbf{F}}s_L\left(\boldsymbol{\Lambda'},t\right)\boldsymbol{n}\left(\boldsymbol{\Lambda'},t\right)\mathbf{H}\left(\boldsymbol{\Lambda}-\boldsymbol{\Lambda'},t\right)d\boldsymbol{\Lambda'}\,. \tag{13}$$

Note that the laminar burning velocity appearing in Eq. (13) cannot be treated as a constant. As discussed earlier, depending on the flame geometry, individual points on the surface, for instance the tip of a trailing cusp, can move substantially faster than the unstrained laminar burning velocity. These singular

points are therefore very important for the dynamics of the flame. Physically, these lead to a removal of flame surface, which will be considered as dissipation terms in the equation for the sub-filter flame front fluctuations derived below. This equation will be used in the model for the sub-filter turbulent burning velocity.

Since the filter changes in time, the filtering operation does not commute with the time derivative. Hence, using this filter, we cannot determine the displacement speed of the filtered position, but only the filtered displacement speed of the instantaneous front. Both would be the same for a commutating filter. To obtain an equation for the filtered flame front location, rather than filtering the G-field, a new level set function $\check{G}$ is introduced that describes the evolution of the filtered flame front location. An implicit representation of the filtered flame surface is given as

$$\check{G}(\widehat{\boldsymbol{x}}_{\boldsymbol{f}}, t) = G_0\,. \tag{14}$$

Differentiation of Eq. (14) leads to

$$\frac{\partial \check{G}}{\partial t} + \frac{d\widehat{\boldsymbol{x}}_f}{dt} \cdot \nabla \check{G} = 0\,. \tag{15}$$

Note here that the $\widehat{\ }$-quantities are a direct result of the filtering operation Eq. (10), whereas $\check{G}$ is not defined as the filtered instantaneous G-field, but is the level set representation of the filtered flame front location. In order to use Eq. (15), the displacement speed of the filtered front appearing in that equation needs to be provided. However, using the filtering operation described in the previous section, this quantity cannot be determined exactly, since the filter kernel does not commute with the time derivative. Here we will therefore use the filtered displacement speed of the unfiltered front given by Eq. (11) as an approximation [17]. This results in

$$\frac{\partial \check{G}}{\partial t} + \widehat{\frac{d\boldsymbol{x}_{\boldsymbol{f}}}{dt}} \cdot \nabla \check{G} = 0\,. \tag{16}$$

This approximation to Eq. (15) is exact, if a commutative filter is used. Introducing Eq. (11) into Eq. (16) yields the G-equation for the mean flame front location as

$$\frac{\partial \check{G}}{\partial t} + \widehat{\boldsymbol{v}} \cdot \nabla \check{G} = -\widehat{s_L \boldsymbol{n}} \cdot \nabla \check{G}\,. \tag{17}$$

It has been shown by Oberlack et al. [13] that as a direct consequence of the symmetries of the G-equation, the model for the propagation term defined in

Eq. (13) has to be proportional to the normal vector of the filtered flame front position

$$\check{\boldsymbol{n}} = -\frac{\nabla \check{G}}{\left|\nabla \check{G}\right|}\,. \tag{18}$$

The propagation term has two contributions, the propagation of the mean front with the filtered laminar burning velocity and the turbulent sub-filter burning velocity s_T. This term can hence be modeled as

$$\widehat{s_L \boldsymbol{n}} = (\widehat{s}_L + s_T)\check{\boldsymbol{n}} = -(\widehat{s}_L + s_T)\frac{\nabla \check{G}}{\left|\nabla \check{G}\right|}\,. \tag{19}$$

The filtered laminar burning velocity, as a conditional average along the sub-filter flame front, can be expressed as

$$\widehat{s}_L = \int\limits_{\boldsymbol{\alpha}} s_L(\boldsymbol{\alpha}) p_{G_0}(\boldsymbol{\alpha}) d\boldsymbol{\alpha}\,. \tag{20}$$

where $\boldsymbol{\alpha}$ represents a vector of parameters influencing the laminar burning velocity. This could include the unburned temperature, the equivalence ratio, and the unburned mixture composition. $p_{G_0}(\boldsymbol{\alpha})$ is the joint probability density function of all α conditioned on the flame front location.

Note that according to the definition of G_0, the conditional velocity is either the filtered velocity in the immediate unburned or burned side of the flame. These will be denoted by $\widehat{\boldsymbol{v}}_u$ and $\widehat{\boldsymbol{v}}_b$, respectively. Similarly, the turbulent burning velocity has to be defined with respect to the unburned or burned gases, denoted by $s_{T,u}$ and $s_{T,b}$. With these notations, depending on the definition of G_0, Eq. (17) can be written as

$$\frac{\partial \check{G}}{\partial t} + \widehat{\boldsymbol{v}}_u \cdot \nabla \check{G} = (\widehat{s}_{L,u} + s_{T,u}) \left|\nabla \check{G}\right| \tag{21}$$

or

$$\frac{\partial \check{G}}{\partial t} + \widehat{\boldsymbol{v}}_b \cdot \nabla \check{G} = (\widehat{s}_{L,b} + s_{T,b}) \left|\nabla \check{G}\right|\,. \tag{22}$$

The evolution of the filtered flame front location can be described by either one of the Eqs. (21) and (22). To solve these equations, models for the sub-filter burning velocity and the flame front conditioned filtered velocity have to be provided. The latter quantity has to be modeled in terms of the Favre-filtered

velocities, which are known from the solution of the Favre-filtered momentum equations. Models for these quantities will be provided in subsequent sections.

4 Model for the conditionally filtered flow velocity

A consistency requirement for the conditional-velocity model is imposed by the equivalence of Eqs. (21) and (22). After applying a model for $\widehat{\boldsymbol{v}}_u$ in Eq. (21) and $\widehat{\boldsymbol{v}}_b$ in Eq. (22), these still have to have the same solution. It is obvious that just replacing the conditional velocities by the unconditional velocities does not satisfy this consistency condition. In the following, we will therefore first develop a model for the conditional velocities, and then show that applying the model to both equations leads to equivalent formulations.

The conditional velocity $\widehat{\boldsymbol{v}}$ is the velocity at the flame front, weighted with the filter function $\mathbf{H}$ and averaged over the entire flame surface within the filter volume. Physically, this averaged velocity, as it appears in the convection term in Eq. (17), leads to the convection of the entire sub-filter flame surface. Hence, it is important only to capture the large-scale velocity motion in the model for the conditional velocities, and not the small scale velocity fluctuations. These only lead to sub-grid flame wrinkling, but not to convection on the resolved scales. Since there typically is a considerable velocity jump across the flame surface, and the velocity jump is assumed to be large compared with the turbulent fluctuations, the local unfiltered velocities will be assumed to be constant in the burned and the unburned part of the sub-filter volume. These velocities are then equal to the respective conditional velocities. This assumption is similar to the Bray-Moss-Libby formalism [1], which has also been employed in the context of LES by Hawkes and Cant [3]. The local velocity can then be approximated as

$$\boldsymbol{v}(G) = \begin{cases} \widehat{\boldsymbol{v}}_u \text{ if } G < G_0 \\ \widehat{\boldsymbol{v}}_u \text{ if } G = G_0 \text{ and } G_0 \text{ defined in the unburned} \\ \widehat{\boldsymbol{v}}_b \text{ if } G = G_0 \text{ and } G_0 \text{ defined in the burned} \\ \widehat{\boldsymbol{v}}_b, \text{ if } G > G_0 \end{cases} , \tag{23}$$

where a distinction has been made, whether G_0 is defined to be in the unburned or the burned mixture. The unconditional Favre-filtered velocity can then be expressed by

$$\overline{\rho}\widetilde{\boldsymbol{v}} = \int_{-\infty}^{\infty} \rho \boldsymbol{v}(G) P(G) dG = \rho_u \widehat{\boldsymbol{v}}_u \int_{-\infty}^{G_0} P(G) dG + \rho_b \widehat{\boldsymbol{v}}_b \int_{G_0}^{\infty} P(G) dG \,, \tag{24}$$

where $P(G)$ is the pdf of finding a particular value of G. Introducing the probability of finding burned mixture p_b as

$$p_b = \int_{G_0}^{\infty} P(G) dG \,, \tag{25}$$

the unconditional velocity can be written as

$$\overline{\rho}\widetilde{\boldsymbol{v}} = \rho_u \widehat{\boldsymbol{v}}_u (1 - p_b) + \rho_b \widehat{\boldsymbol{v}}_b p_b \,. \tag{26}$$

Similarly, the unconditionally filtered density can be derived as

$$\overline{\rho} = \rho_u (1 - p_b) + \rho_b p_b \,. \tag{27}$$

To express $\widehat{\boldsymbol{v}}_b$ by $\widehat{\boldsymbol{v}}_u$, we will use the jump condition for the mass balance across the mean flame interface, given by

$$\rho_u \check{\boldsymbol{n}} \cdot \left(\widehat{\boldsymbol{v}}_u - \widehat{\frac{d\boldsymbol{x_f}}{dt}} \right) = \rho_b \check{\boldsymbol{n}} \cdot \left(\widehat{\boldsymbol{v}}_b - \widehat{\frac{d\boldsymbol{x_f}}{dt}} \right) . \tag{28}$$

The displacement speed can be expressed by Eq. (11), where the choice of the conditional velocity and the burning velocity depend on the location of G_0 with respect to the flame. If G_0 is defined to be in the unburned mixture, $\widehat{\boldsymbol{v}}_u$ and $s_{T,u}$ have to be used. However, if G_0 is in the burned gases, then the appropriate values are given by $\widehat{\boldsymbol{v}}_b$ and $s_{T,b}$. For the velocity jump across the flame front this results in

$$\check{\boldsymbol{n}} \cdot (\widehat{\boldsymbol{v}}_u - \widehat{\boldsymbol{v}}_b) = \frac{\rho_u - \rho_b}{\rho_b} \check{\boldsymbol{n}} \cdot (\widehat{s_L \boldsymbol{n}})_u \,, \tag{29}$$

if G_0 is defined to be in the unburned mixture, and

$$\check{\boldsymbol{n}} \cdot (\widehat{\boldsymbol{v}}_u - \widehat{\boldsymbol{v}}_b) = \frac{\rho_u - \rho_b}{\rho_u} \check{\boldsymbol{n}} \cdot (\widehat{s_L \boldsymbol{n}})_b \,, \tag{30}$$

if G_0 is in the burned gases. Both of these relations can now be used with Eq. (26) to derive a model for the conditional velocities $\widehat{\boldsymbol{v}}_u$ and $\widehat{\boldsymbol{v}}_b$. Here only the former will be shown. Introducing Eq. (29) into Eq. (26) results in an expression for the conditional velocity in terms of the unconditional velocity as

$$\check{\boldsymbol{n}} \cdot \widehat{\boldsymbol{v}}_u = \check{\boldsymbol{n}} \cdot \widetilde{\boldsymbol{v}} + \frac{\rho_u - \rho_b}{\overline{\rho}} \check{\boldsymbol{n}} \cdot (\widehat{s_L \boldsymbol{n}})_u p_b \,. \tag{31}$$

In order to make use of this relation in the G-equation given by Eqs. (21) and (22), we first split the convection term into a flame normal and a flame tangential part. Since the flame tangential part only leads to a parallel translation of the flame front and has no influence on the flame propagation, it can be neglected. The convection term from Eq. (21) can then be written as

$$\widehat{\boldsymbol{v}}_u \cdot \nabla \check{G} = (\check{\boldsymbol{n}} \cdot \widehat{\boldsymbol{v}}_u)\, \check{\boldsymbol{n}} \cdot \nabla \check{G}\,. \tag{32}$$

After introducing Eq. (31) into the normal convection term given by Eq. (32), only the normal component of the unconditional velocity appears, which can again be complemented by the tangential part without changing the solution. This leads to

$$\frac{\partial \check{G}}{\partial t} + \widetilde{\boldsymbol{v}} \cdot \nabla \check{G} = -\left(1 + \frac{\rho_u - \rho_b}{\overline{\rho}} p_b\right) (\widehat{s_L \boldsymbol{n}})_u \cdot \nabla \check{G}\,. \tag{33}$$

With Eq. (27), the equation for the filtered flame front position can then be written as

$$\frac{\partial \check{G}}{\partial t} + \widetilde{\boldsymbol{v}} \cdot \nabla \check{G} = -\frac{\rho_u}{\overline{\rho}} (\widehat{s_L \boldsymbol{n}})_u \cdot \nabla \check{G}\,. \tag{34}$$

Using the expression for the filtered propagation term from Eq. (19) results in

$$\frac{\partial \check{G}}{\partial t} + \widetilde{\boldsymbol{v}} \cdot \nabla \check{G} = \frac{\rho_u}{\overline{\rho}} (\widehat{s}_{L,u} + s_{T,u}) \left|\nabla \check{G}\right|\,. \tag{35}$$

Similarly, starting by introducing Eq. (30) into Eq. (26), the equation with G_0 defined in the burnt gases can be derived as

$$\frac{\partial \check{G}}{\partial t} + \widetilde{\boldsymbol{v}} \cdot \nabla \check{G} = \frac{\rho_b}{\overline{\rho}} (\widehat{s}_{L,b} + s_{T,b}) \left|\nabla \check{G}\right|\,. \tag{36}$$

It is easily seen that these equations satisfy some important limits. If Eq. (34) is evaluated in the unburned mixture, then $\widetilde{\boldsymbol{v}} = \widehat{\boldsymbol{v}}_u$ and $\overline{\rho} = \rho_u$. Hence, Eq. (21) is recovered. If, on the other hand, this equation is evaluated in the burned gases, $\widetilde{\boldsymbol{v}} = \widehat{\boldsymbol{v}}_b$, $\overline{\rho} = \rho_b$, the right hand side becomes $(\widehat{s}_{L,b} + s_{T,b}) \left|\nabla \check{G}\right|$, since the mass conservation through the flame requires

$$\rho_u (\widehat{s}_{L,u} + s_{T,u}) = \rho_b (\widehat{s}_{L,b} + s_{T,b})\,. \tag{37}$$

Therefore, in the burned gases, Eq. (22) is recovered. By using Eq. (37), it can also be shown easily that Eqs. (35) and (36) are equivalent.

5 *G*-equation for the filtered flame location valid in the corrugated flamelets and the thin reaction zones regime

In the derivation for the instantaneous G-equation for the thin reaction zones regime, Peters [2,12] starts from the instantaneous temperature equation and develops a level set equation for a temperature iso-surface given by $T(\boldsymbol{x},t) = T^0$, where T^0 is the inner layer temperature. The expression for the propagation speed is similar to Eq. (3), where, following [18], the displacement speed, s_d, can be written as

$$s_d = \left(\frac{\nabla \cdot (\rho D \nabla T) + \omega_T}{\rho |\nabla T|} \right)_{T=T^0} . \tag{38}$$

Here, ρ is the density, D is the temperature diffusivity, and ω_T is the chemical source term. With the temperature iso-surface normal vector $\boldsymbol{n}_T = -\nabla T/|\nabla T|$, the transport term in Eq. (38) can be expressed by its components normal and tangential to the T^0 surface [19] and the displacement speed becomes

$$\begin{aligned} s_d &= -\left(D \nabla \cdot \boldsymbol{n}_T\right)_{T=T^0} + \left(\frac{-\boldsymbol{n}_T \left(\rho D |\nabla T|\right) - \omega_T}{|\nabla T|} \right)_{T=T^0} && (39) \\ &= s_\kappa + (s_n + s_r) . && (40) \end{aligned}$$

Peters et al. [20] have shown that $(s_n + s_r)$, which for unstrained premixed flames corresponds to the laminar burning velocity, is not significantly changed by turbulence, and therefore, in the thin reaction zones regime, is small compared with the contribution from curvature s_κ. Since the temperature iso-surface $T = T^0$ will be described by $G = G_0$, s_κ can be written as

$$s_\kappa = -D \nabla \cdot \boldsymbol{n} = D \nabla \cdot \left(\frac{\nabla G}{|\nabla G|} \right) . \tag{41}$$

The combined displacement velocity valid in the corrugated flamelets and the thin reaction zones regime is given by an expression similar to Eq. (3), but with the laminar burning velocity s_L replaced by $s_L + s_\kappa$. Filtering this expression with the filtering operation given by Eq. (10) leads to

$$\widehat{\frac{d\boldsymbol{x_f}}{dt}} = \widehat{\boldsymbol{v}} + \widehat{(s_L + s_\kappa)\,\boldsymbol{n}} . \tag{42}$$

Introducing Eq. (42) into Eq. (16) leads to the G-equation valid for the corrugated flamelets and the thin reaction zones regime

$$\frac{\partial \check{G}}{\partial t} + \widehat{\boldsymbol{v}} \cdot \nabla \check{G} = -\widehat{(s_L + s_\kappa)\,\boldsymbol{n}} \cdot \nabla \check{G}\,. \tag{43}$$

Before proposing a model for the burning velocity, we have to discuss the thin reaction zones regime in the context of LES using the LES regime diagram. The diagram shown in Fig. 2 is essentially the same as that given by Pitsch and Duchamp [6], but has one additional line. The diagram shows the ratio of LES filter width Δ to the laminar flame thickness l_F over the Karlovitz number Ka defined as

$$\mathrm{Ka} = \frac{t_c}{t_\eta} = \frac{l_F^2}{\eta^2} = \left(\frac{u_\Delta'^3 l_F}{s_L^3 \Delta}\right)^{1/2}\,, \tag{44}$$

where η is the Kolmogorov length scale, t_η denotes the Kolmogorov time scale, and u'_Δ is the sub-filter velocity fluctuation. Ka_δ, which also appears in the diagram, is the Karlovitz number based on the inner layer thickness δ instead of on the Kolmogorov scale. The sub-filter Reynolds number is defined as $\mathrm{Re}_\Delta = u'_\Delta \Delta / s_L l_F$.

The corrugated flamelets, the thin reaction zones, and the broken reaction zones regimes are separated by constant Ka lines. The corrugated flamelets area is separated from the wrinkled flamelets area by the $\Delta = l_G$ line, where l_G is the Gibson scale. It is important to note that this distinction here does not constitute a difference in the turbulence/chemistry interaction. At this point, the filter size simply becomes smaller than the Gibson scale, which is the smallest turbulent scale of the flame front wrinkling. Hence, in the wrinkled flamelets region, all flame wrinkling is resolved and a sub-filter model for the turbulent flame front wrinkling is not required. Also in the thin reaction zones regime, there appears a similar distinction marked by the $\mathrm{Da}_\Delta = 1$ line. The sub-filter Damköhler number is defined as

$$\mathrm{Da}_\Delta = \frac{s_L \Delta}{u'_\Delta l_F}\,. \tag{45}$$

The physical meaning of this will be discussed next. In the thin reaction zones regime, the Kolmogorov scale is smaller than the laminar flame thickness l_F, but still larger than the inner layer thickness δ. The reaction zone structure therefore stays intact, but the turbulence broadens the preheat region and increases the mixing process. In analogy to laminar flames, where the flame thickness is given by $l_F = \sqrt{D t_c}$, Peters [12] suggested that the broadened flame thickness in this regime, l_m, can be determined as the characteristic

length scale of the turbulent eddy with a characteristic time equal to the chemical time scale. This assumption leads to $l_m^2 = \varepsilon t_c^3$, where ε is the turbulent kinetic energy dissipation rate. With $\varepsilon = u_\Delta'^3/\Delta$ and $t_c = l_F/s_L$ follows

$$\frac{l_m}{\Delta} = \left(\frac{u'_\Delta l_F}{s_L \Delta}\right)^{3/2} = \mathrm{Da}_\Delta^{-3/2} \,. \tag{46}$$

The Da_Δ =1 line can be found in the regime diagram from the relation

$$\mathrm{Da}_\Delta = \mathrm{Ka}^{-2/3} \frac{\Delta}{l_F}^{2/3} \,. \tag{47}$$

Equation 46 implies that if $\mathrm{Da}_\Delta > 1$, which is to the left of the $\mathrm{Da}_\Delta = 1$ line indicated in Fig. 2, the entire flame region is smaller than the filter size and the entire temperature change from unburnt to burnt occurs on the sub-filter scale. If, on the other hand, $\mathrm{Da}_\Delta < 1$, the turbulent preheat region is larger than the filter size and the temperature change has to occur on the resolved scale. It also implies that the mixing in the preheat region partly occurs on the resolved scale.

This leads to an important difference in the modeling of the G-equation for the mean flame front position and, for instance, a filtered temperature equation. For the temperature equation, the turbulent mixing of the temperature field occurring on the resolved scale is computed directly, only the sub-filter mixing has to be modeled. For the G-equation this is different. The effect of the resolved mixing on the front propagation also has to be modeled.

The propagation term in the equation for the mean flame front position has contributions from s_L and $s_\kappa = D\kappa$, where κ is the front curvature. In the model for the propagation term, described below, for the s_L term, a resolved and a sub-filter part have to be considered. This part of the model is equivalent to the model used for the corrugated flamelets regime. The s_κ term arises from the interaction of transport in the preheat region of the flame with the flame curvature. The model proposed below accounts for the interactions of molecular mixing and resolved curvature, the interaction of sub-filter turbulent transport within the flame and the sub-filter curvature, and the interaction of the sub-filter turbulent transport with the resolved curvature. The model for the front propagation is given as

$$\widehat{(s_L + s_\kappa)\,\boldsymbol{n}} = (\widehat{s}_L + s_T - D\check{\kappa} - D_{t,\kappa}\check{\kappa})\,\check{\boldsymbol{n}} \,, \tag{48}$$

where it is assumed that the molecular diffusivity is a function of the temperature only. Then, the conditionally filtered value can be replaced by its value at the inner layer temperature.

The first part of the model is the propagation of the mean front with the filtered laminar burning velocity, which similarly appeared in Eq. (19). The third term describes the interaction of molecular transport with the resolved curvature. These terms have to be included in the model to recover the laminar limit in the resolved turbulence regime. The second term accounts for all terms that occur entirely on the sub-filter scale. This includes the sub-filter propagation by the laminar burning velocity and the interaction of sub-filter turbulent transport and sub-filter curvature. The fourth term describes the interaction of the sub-filter turbulent transport with the resolved curvature. The models of these terms will be discussed in the following.

In the thin reaction zones regime, modeling of curvature effects becomes important. Turbulent mixing in the preheat region in combination with flame front curvature leads to scalar dissipation and to a removal of flame front wrinkling, which leads to an enhanced propagation speed. As discussed above, for $\mathrm{Da}_\Delta > 1$, the entire flame is on the sub-filter scale. This interaction of sub-filter turbulent transport and unresolved curvature appears in the turbulent burning velocity s_T. The modeling of this quantity is described below.

The interaction of mixing in the flame preheat region with the flame front curvature is most important if the flame thickness is equal to the curvature radius. However, mixing also interacts with larger curvature radii, although the effect becomes less important. The fourth term in the model for the mean front propagation, Eq. (48), accounts for interactions of the turbulent sub-filter mixing in the preheat region with the resolved curvature. The turbulent length scale responsible for mixing in the preheat region is l_m. From this follows that the turbulent diffusivity that causes mixing in the preheat region of the flame can be modeled as

$$D_{t,\kappa} = \frac{c_\nu}{\mathrm{Sc}_t} u'_m l_m \,, \tag{49}$$

where Sc_t is the turbulent Schmidt number, c_ν is a constant, and u'_m is the characteristic velocity fluctuation of a turbulent eddy of length scale l_m. Using Kolmogorov scaling, u'_m can be expressed as

$$u'_m = u'_\Delta \left(\frac{l_m}{\Delta}\right)^{1/3} \,, \tag{50}$$

and for $D_{t,\kappa}$ follows with Eq. (46)

$$D_{t,\kappa} = \frac{c_\nu}{\mathrm{Sc}_t} u'_\Delta \Delta \left(\frac{l_m}{\Delta}\right)^{4/3} = D_t \mathrm{Da}_\Delta^{-2} \,, \tag{51}$$

where it has been assumed that the turbulent Schmidt number and the coefficient c_ν are scale independent. Equation (51) is valid if $l_m < \Delta$, which means $\mathrm{Da}_\Delta > 1$. For large Damköhler number, the broadened flame thickness becomes small compared to the resolved curvature, and the interaction becomes negligible. For $\mathrm{Da}_\Delta < 1$, l_m becomes larger than the curvature radius, and the preheat zone mixing length can no longer interact with the smallest resolved curvature. Only length scales comparable to the curvature radius or smaller can interact. Hence, for $\mathrm{Da}_\Delta < 1$, $D_{t,\kappa}$ has to be modeled as

$$D_{t,\kappa} = D_t \,. \tag{52}$$

With Eqs. (51) and (52), Eq. (48) becomes

$$\widehat{(s_L + s_\kappa)\,\boldsymbol{n}} = \left(\widehat{s}_L - D\check{\kappa} + s_T - D_t \mathrm{Da}_\Delta^{-2}\check{\kappa}\right)\check{\boldsymbol{n}}\,, \tag{53}$$

for $\mathrm{Da} > 1$, and

$$\widehat{(s_L + s_\kappa)\,\boldsymbol{n}} = (\widehat{s}_L - D\check{\kappa} + s_T - D_t\check{\kappa})\,\check{\boldsymbol{n}}\,, \tag{54}$$

otherwise [1] .

This is slightly different from the model proposed by Peters [2] for RANS and formulated by Pitsch and Duchamp [6] for LES. Here, because of the appearance of the Damköhler number, the curvature term vanishes for $\mathrm{Da}_\Delta \gg 1$, and hence, also in the limit of the corrugated flamelets regime. This is in agreement with the findings of Oberlack et al. [13] who demonstrated in the corrugated flamelets regime that this form of the model is consistent with invariant modeling. Note that the resolved curvature term can be negative or positive, depending on the sign of the resolved curvature. Because of this, the resolved curvature term always leads to a stabilization of the mean flame front by removing flame front wrinkling.

The model for the conditional velocity given in Eq. (31) is not strictly valid in the thin reaction zones regime. The jump condition in Eq. (28) used in the derivation of Eq. (31) cannot be applied because of the thickening of the

[1] This model can similarly be formulated for the G-equation for the mean flame front position in the Reynolds averaged context, leading to Eq. (51) with the filter scale quantities replaced with those at the integral scales of the turbulence. Then, also the Damköhler number is based on the integral scales of the turbulence, and the condition $\mathrm{Da}_\Delta < 1$ implies a mixing length l_m larger than the integral length scale of the turbulence. The integral scale is the largest scale to be considered in the mixing, and hence, for $\mathrm{Da}_\Delta < 1$, Eq. (52) applies.

preheat region. However, at least for $\mathrm{Da}_\Delta > 1$, Eq. (31) might still be a good approximation, because the temperature change occurs on a scale smaller than the filter size. For Da_Δ <1, the thickness of the preheat region is larger than the filter size and the jump condition is no longer valid. However, the model at least preserves the mass flux consistency discussed at the end of the section describing the model for the conditional velocity and can therefore still be used as an approximation for the conditional velocity even for $\mathrm{Da}_\Delta < 1$.

6 Equation for the sub-filter flame brush thickness

We now want to derive an equation for the length-scale of the sub-filter flame front fluctuations l, which might be associated with the sub-filter flame brush thickness. This equation will then be used to derive a model for the sub-filter turbulent burning velocity. Different definitions for l are possible. A reasonable way to determine the flame front fluctuation is to determine l as the distance of the instantaneous to the filtered flame front at a given value of $\mathbf{\Lambda}$. This corresponds to the definition used in Oberlack et al. [13] and is schematically shown in Fig. 3. The sub-filter flame front fluctuation could then be written as

$$l = |\boldsymbol{l}| \qquad \text{with} \qquad \boldsymbol{l} = \boldsymbol{x_f} - \widehat{\boldsymbol{x}}_f \,. \tag{55}$$

However, for the derivation of a transport equation for this quantity, a filtering operation that commutes with the time derivative has to be used. As noted earlier, the filter defined in Eq. (10) does not possess this property. We will therefore define the length scale through the dynamics of the flame front. This is consistent with the derivation of the level set equation for the mean flame front position, Eq. (17). The rate of change of $\boldsymbol{l}$ at a given value of $\mathbf{\Lambda}$ is given by the difference of the displacement speed of the instantaneous front and the filtered displacement speed of the instantaneous front. This can be written as

$$\frac{d\boldsymbol{l}}{dt} = \frac{d\boldsymbol{x_f}}{dt} - \widehat{\frac{d\boldsymbol{x_f}}{dt}} \tag{56}$$

with the initial condition given by Eq. (55). For a commutative filtering operation, this corresponds to the definition in Eq. (55).

Similar to the G-variance equation given in Peters [2], the equation for flame front fluctuations has a production term, active on the large scales, and two dissipation terms: the kinematic restoration term, important in the corrugated flamelets regime, and the scalar dissipation term, important in the thin reaction zones regime. The length scale equation should therefore be derived

and modeled separately in each of these regimes and combined subsequently. Here, for brevity, only the combined equation, valid in both regimes, will be derived. However, the modeling of each dissipation term will be done in the limits, where only one of the dissipation terms is important.

An expression for $\boldsymbol{l}$ can be derived from Eq. (56) using Eq. (42) and the corresponding unfiltered equation as

$$\frac{d\boldsymbol{l}}{dt} = \boldsymbol{v} - \widehat{\boldsymbol{v}} + s_L\boldsymbol{n} - \widehat{s_L\boldsymbol{n}} + s_\kappa\boldsymbol{n} - \widehat{s_\kappa\boldsymbol{n}}\,. \tag{57}$$

The equation for the length scale of the sub-filter flame front fluctuations can then be obtained by multiplying Eq. (57) with $\boldsymbol{l}$ and applying the filtering operation, given by Eq. (10). This leads to

$$\widehat{\frac{dl^2}{dt}} = 2\widehat{\boldsymbol{l}\cdot\boldsymbol{v'}} + 2\widehat{\boldsymbol{l}\cdot(s_L\boldsymbol{n})'} + 2\widehat{\boldsymbol{l}\cdot(s_\kappa\boldsymbol{n})'}\,, \tag{58}$$

where the sub-filter velocity fluctuation has been introduced as $\boldsymbol{v'} = \boldsymbol{v} - \widehat{\boldsymbol{v}}$ and the turbulent burning velocity fluctuations as $(s_L\boldsymbol{n})' = s_L\boldsymbol{n} - \widehat{s_L\boldsymbol{n}}$ and $(s_\kappa\boldsymbol{n})' = s_\kappa\boldsymbol{n} - \widehat{s_\kappa\boldsymbol{n}}$. The physical meaning of Eq. (58) is similar to the σ-equation provided by Peters [12]. Hence, also the source and sink terms appearing in these equations have the same physical origin and the same arguments are used here for their modeling. In Eq. (58), the term on the left hand side describes the rate of change of the length scale following the flame front. The first term on the right hand side describes the production of flame front wrinkling due to the turbulence, whereas the second and third terms on the right hand side are the flame surface dissipation due to flame propagation and diffusive curvature effects, respectively.

To model the production term in Eq. (58), we have to consider the scalar flux term $\widehat{\boldsymbol{l}\cdot\boldsymbol{v'}}$, which would typically be expressed using a gradient transport assumption, involving a turbulent eddy viscosity and the spatial gradient of the scalar. However, since the flame front fluctuation l is defined at the mean flame front position only, spatial gradients of this quantity are not defined. If the flame front is in steady state with the turbulence, the sub-filter wrinkling l has to be of order of a sub-filter turbulent length scale, which can be expressed as $c_S\Delta$, where c_S is the Smagorinski constant. The production term can then be modeled as

$$\widehat{\boldsymbol{l}\cdot\boldsymbol{v'}} = c_1 c_S \Delta v'_\Delta = \frac{c_1\nu_{t,\Delta}}{c_\nu}\,, \tag{59}$$

where c_ν is a proportionality constant and ν_t is the sub-filter eddy viscosity given by $\nu_{t,\Delta} = c_\nu c_S \Delta v'_\Delta$. Note that for the production of the flame wrinkling

the largest sub-filter turbulent length scale is important, while in the earlier discussion on the interaction of the turbulent transport within the flame with the resolved curvature, the flame thickness l_m was the important scale.

Since both dissipation terms act on the small scales, the scaling relations for these terms provided by Peters [12] in a Reynolds averaged context can also be applied here. In the corrugated flamelets regime, the kinematic restoration term is the dominant dissipation term. This term should be independent of small scale quantities such as the laminar burning velocity. It scales with the mean propagation term important in the corrugated flamelets regime, given by Eq. (19), and can be expressed as

$$\widehat{\boldsymbol{l} \cdot (s_L \boldsymbol{n})'} = -c_2 c_S \Delta \, \check{\boldsymbol{n}} \cdot \widehat{s_L \boldsymbol{n}} = -c_2 c_S \Delta \, s_T \,, \tag{60}$$

where the unresolved part of the turbulent burning velocity has been introduced as $\widehat{s_L \boldsymbol{n}} = s_T \check{\boldsymbol{n}}$.

Similarly, also the scalar dissipation term, dominant in the thin reaction zones regime, is assumed to scale with the respective sub-filter mean propagation term. Since a dissipation term can be written independently of the large scales, the missing length scale is obtained from the small scale quantities and it follows

$$\widehat{\boldsymbol{l} \cdot (s_\kappa \boldsymbol{n})'} = -c_3 \frac{l_F}{s_L} \left(\check{\boldsymbol{n}} \cdot \widehat{s_\kappa \boldsymbol{n}} \right)^2 = -c_3 \frac{l_F}{s_L} s_T^2 \,. \tag{61}$$

For both Eqs. (60) and (61), the resolved contributions have not been considered, since these are explicitly included in the model given by Eq. (48).

Introducing Eqs. (59), (60), and (61) into Eq. (58), and assuming that production equals dissipation in that equation, an expression for the turbulent burning velocity can be obtained as

$$\frac{c_1 \nu_{t,\Delta}}{c_\nu} - c_2 c_S \Delta \, s_T - c_3 \frac{l_F}{s_L} s_T^2 = 0 \,. \tag{62}$$

This leads to

$$\frac{s_T}{s_L} = -\frac{b_3^2 c_\nu c_S \Delta s_L}{2 b_1 \mathrm{Sc}_t D} + \sqrt{\left(\frac{b_3^2 c_\nu c_S \Delta s_L}{2 b_1 \mathrm{Sc}_t D} \right)^2 + \frac{b_3^2 \nu_t}{\mathrm{Sc}_t D}} \,. \tag{63}$$

Here, the constants c_2/c_3 and c_1/c_3 have been determined such that Eq. (63) results for $\Delta/l_F \to \infty$ in Damköhler's large-scale limit

$$\frac{s_T}{s_L} = b_1 \frac{v'_\Delta}{s_L}\,, \tag{64}$$

and for $\Delta/l_F \to 0$ in the small-scale limit

$$\frac{s_T}{s_L} = b_3 \sqrt{\frac{D_t}{D}}\,. \tag{65}$$

The resulting expressions for the constants are $c_2/c_3 = c_\nu b_3^2 s_L l_F/(b_1 \mathrm{Sc}_t) D$ and $c_1/c_3 = c_\nu b_3^2 s_L l_F/(\mathrm{Sc}_t\ \mathrm{D})$, where the constants b_1 and b_3 can be taken from Peters [2] to be $b_1 = 2.0$ and $b_3 = 1.0$. The turbulent sub-filter Schmidt number $\mathrm{Sc}_t = \nu_t/D_t$ can be determined using a dynamic model. Alternatively, a constant value of $\mathrm{Sc}_t = 0.4$ can be used [21].

To avoid the use of the Smagorinsky coefficient and the constant c_ν, the model can alternatively be written as

$$\frac{s_T}{s_L} = -\frac{b_3^2}{2 b_1 \mathrm{Sc}_t} \frac{\nu_t}{D} \frac{s_L}{v'_\Delta} + \sqrt{\left(\frac{b_3^2}{2 b_1 \mathrm{Sc}_t} \frac{\nu_t}{D} \frac{s_L}{v'_\Delta} \right)^2 + \frac{b_3^2 \nu_t}{\mathrm{Sc}_t D}}\,. \tag{66}$$

The model given by Eqs. (63) or (66) is similar to the expression derived by Peters [12] in the RANS context, since the same physical arguments have been used in the derivation. The expression can alternatively be written as a simple function of the Da number. Here, it has been kept in the present form to facilitate the numerical evaluation. A direct validation of this expression for LES is non-trivial. However, the predicted burning velocities have been shown to agree well with experimental data in the RANS context [2, 12].

Finally, in light of these results, the scaling used in the modeling of the dissipation terms in the length scale equation should be discussed. To derive the models given in Eqs. (60) and (61), dimensional arguments have been used, which, if used differently, could also have led to different results. In particular, for the kinematic restoration, a linear dependence of the propagation term has been assumed, while for the scalar dissipation term a quadratic dependence is used. As an example, for a different scaling possibility, the latter could also have been expressed as linearly dependent on the propagation term times the small scale length scale l_F. Such a scaling has been used in Pitsch and Duchamp [6], which then led to a similar, but different expression for the turbulent burning velocity. The quadratic relation, which, for the scaling used in this study, is given by Eq. (62), then has no linear term, and can be

solved more easily. However, the choice of the particular scaling used here and also in Peters [2] is motivated by results from direct numerical simulations by Wenzel [22], who studied the evolution of the G-equation in forced isotropic turbulence. The scaling of the dissipation terms in the length scale equation has not been investigated, but the scaling of the corresponding terms in an equation for the flame surface area ratio $\sigma = |\nabla G|$ has been given. It has been found that the kinematic restoration term depends quadratically, the scalar dissipation rate cubicly on σ. These dependencies can be translated to the length scale equation. Since $\sigma \sim G'$, it follows that $\frac{dG'^2}{G'^2} \sim \frac{d\sigma}{\sigma}$, which, using $l = \frac{G'}{|\nabla \tilde{G}|}$, leads to $dl^2 = \frac{G'^2}{\sigma} d\sigma$. This shows that compared with the transport equation for σ given in Peters [2], in the equation for l^2, given by Eq. (58), the power of σ in the dissipation terms should be decreased by one. This results in the scaling employed in Eqs. (60) and (61), since, using the present filtering procedure, σ appears in form of the normal vector.

7 Conclusions

This paper provides a consistent level set formulation for LES of premixed turbulent combustion. The governing level set equation for the mean flame front location is derived using a new filtering technique, and models for the flame front conditional velocity and the propagation term are provided. The propagation term consists of essentially four different contributions, the resolved propagation and curvature terms, a sub-filter term, and one term accounting for the interaction of sub-filter transport with resolved curvature, which becomes small for large sub-filter Damköhler number, and becomes important otherwise.

In the application of this model in LES, the filtered density has to be determined from the mean flame front position. This procedure has been described by Pitsch and Duchamp [6]. However, it has been pointed out above that the thickness of the preheat region in the thin reaction zones regime, which is broadended by turbulent mixing, becomes larger than the filter size for sub-filter Damköhler numbers smaller than unity. This implies that in this regime, mixing of the scalar field at the resolved scale has to be considered, and although the model proposed here can be used as an approximation, a more appropriate method has to be developed in the future.

8 Acknowledgments

The author gratefully acknowledge funding by the Air Force Office of Scientific Research. The author also thanks Marcus Herrmann, Seung Hyun Kim, and Evatt R. Hawkes for many inspiring discussions and valuable comments.

References

[1] K. N. C. Bray, P. A. Libby, J. B. Moss, Unified modeling approach for premixed turbulent combustion. 1. General formulation, Combust. Flame 61 (1985) 87–102.

[2] N. Peters, Turbulent Combustion, Cambridge University Press, 2000.

[3] E. R. Hawkes, R. S. Cant, A flame surface density approach to large-eddy simulation of premixed turbulent combustion, Proc. Combust. Inst. 28 (2000) 51–58.

[4] W. W. Kim, S. Menon, Numerical modeling of turbulent premixed flames in the thin-reaction-zones regime, Comb. Sci. Tech. 160 (2000) 119–150.

[5] V. K. Chakravarthy, S. Menon, Large-eddy simulation of turbulent premixed flames in the flamelet regime, Comb. Sci. Tech. 162 (2001) 175.

[6] H. Pitsch, L. Duchamp de Lageneste, Large-eddy simulation of premixed turbulent combustion using a level-set approach, Proc. Combust. Inst. 29 (2002) 2001–2008.

[7] F. Colin, D. Veynante, T. Poinsot, A thickened flame model for large eddy simulation of premixed turbulent combustion, Phys. Fluids 12 (7) (2000) 1843–1863.

[8] C. Nottin, R. Knikker, M. Boger, D. Veynante, Large-eddy simulation of an acoustically excited turbulent premixed flame, Proc. Combust. Inst. 28 (2000) 67–73.

[9] R. Knikker, D. Veynante, C. Meneveau, A priori testing of a similarity model for large eddy simulations of turbulent premixed combustion, Proc. Combust. Inst. 29 (2002) 2105–2111.

[10] F. A. Williams, Turbulent combustion, in: J. D. Buckmaster (Ed.), The Mathematics of Combustion, Society for Industrial & Applied Mathematics, 1985, pp. 197–1318.

[11] N. Peters, A spectral closure for premixed turbulent combustion in the flamelet regime, J. Fluid Mech. 242 (1992) 611–629.

[12] N. Peters, The turbulent burning velocity for large scale and small scale turbulence, J. Fluid Mech. 384 (1999) 107–132.

[13] M. Oberlack, H. Wenzel, N. Peters, On symmetries and averaging of the G-equation for premixed combustion, Comb. Theory Modelling 5 (4) (2001) 1–20.

[14] S. B. Pope, The evolution of surfaces in turbulence, J. Eng. Sci. 26 (1988) 445–469.

[15] E. R. Hawkes, Large eddy simulation of premixed turbulent combustion, Ph.D. thesis, University of Cambridge (2000).

[16] P. J. Colucci, F. A. Jaberi, P. Givi, S. B. Pope, Filtered density function for large eddy simulation of turbulent reacting flows, Phys. Fluids 10 (2) (1998) 499–515.

[17] M. Herrmann, private communication (2005).

[18] C. H. Gibson, Fine structure of scalar fields mixed ty turbulence. I. Zero-gradient points and minimal gradient surfaces, Phys. Fluids 11 (1968) 2305.

[19] T. Echekki, J. H. Chen, Analysis of the contribution of curvature to premixed flame propagation, Comb. Flame 118 (1999) 308–311.

[20] N. Peters, P. Terhoeven, J. H. Chen, T. Echekki, Statistics of flame displacement speeds from computations of $2-d$ unsteady methane-air flames, Proc. Combust. Inst. 27 (1998) 833–839.

[21] H. Pitsch, H. Steiner, Large-eddy simulation of a turbulent piloted methane/air diffusion flame (Sandia flame D), Phys. Fluids 12 (10) (2000) 2541–2554.

[22] H. Wenzel, Direkte numerische Simulation der Ausbreitung einer Flammenfront in einem homogenen Turbulenzfeld, Ph.D. thesis, RWTH Aachen (2000).

List of Figures

Figures

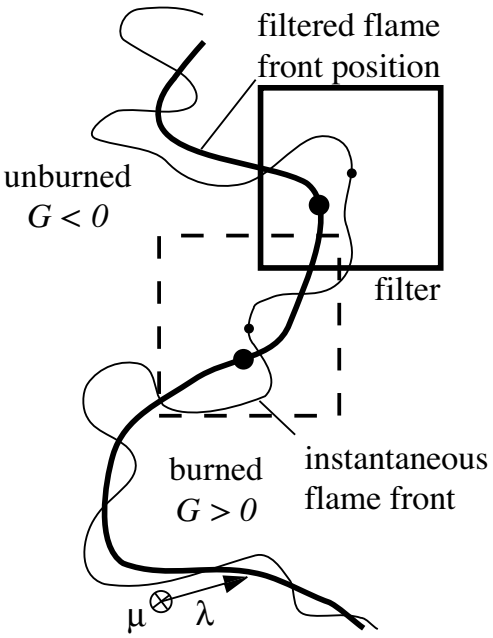

Fig. 1. Instantaneous and filtered flame front position. The rectangle indicates the filter box, which is attached to the instantaneous front at the location indicated by the small circle. The large circle indicates the corresponding filtered flame front position. The dashed rectangle shows the filter at a different λ-position.

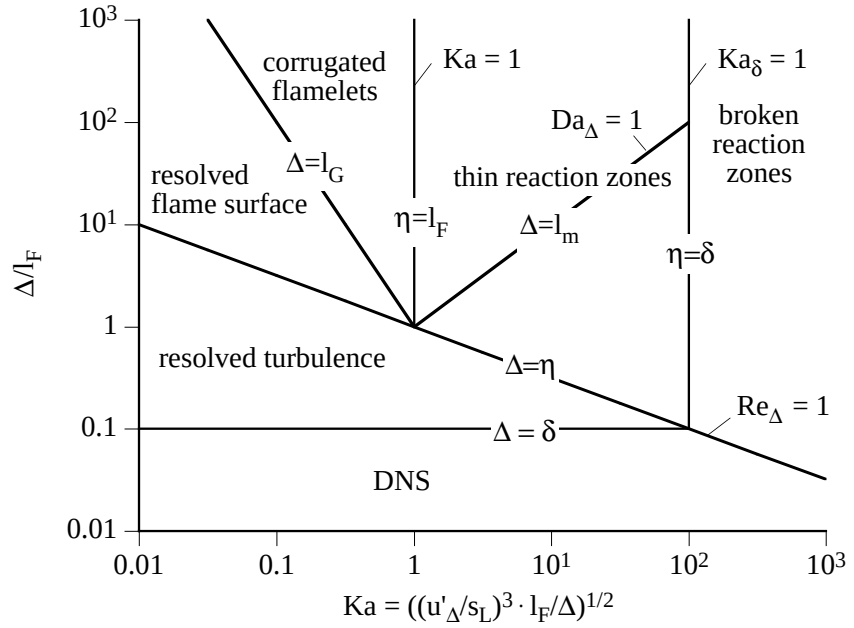

Fig. 2. Regime diagram for LES and DNS of premixed turbulent combustion

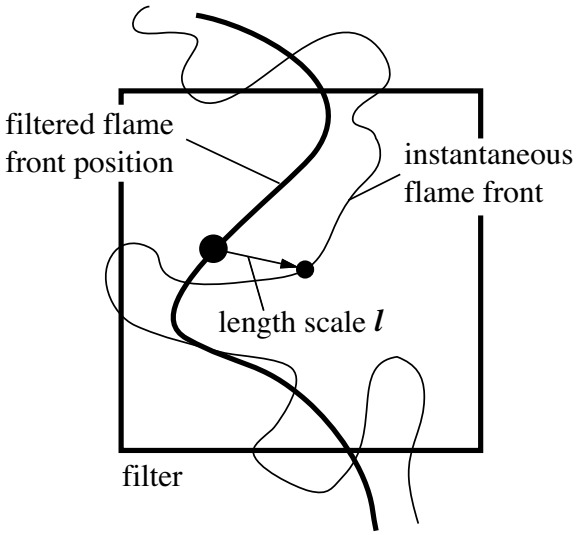

Fig. 3. Instantaneous and filtered flame front position